Accuracy Assessment of Artificial Neural Networks as Viable Techniques for Predicting Open Pit Mine Wall Deformation

[1]Apraku, E. K., [2]Ziggah, Y. Y. and [2]Kumi-Boateng, B.
[1]Goldfields Ghana Limited, Tarkwa, Ghana
[2]University of Mines and Technology, Tarkwa, Ghana

Apraku, E. K., Ziggah, Y. Y. and Kumi-Boateng, B. (2022), "Accuracy Assessment of Artificial Neural Networks as Viable Techniques for Predicting Open Pit Mine Wall Deformation", *Proceeding of the 7th UMaT Biennial International Mining and Mineral Conference*, Tarkwa, Ghana, pp. 1-9.

Abstract

Aside from the traditional statistical regression methods, there have been upsurges in using Artificial Intelligence (AI) techniques for predicting and analysing deformations on tunnels, dams, bridges and subways. This upsurge is linked to the self-adaptive nature of the AI to learn and generalize adequately on the dataset yielding good prediction results. However, little AI predictive analytic works on open pit wall deformation based on geodetic measurements have been done in the mining industry where prediction of active pit wall deformation, if not properly evaluated, can be catastrophic, leading to loss of life, property damage and eventual collapse of mining operations. This paper presents a comparative study of three supervised Artificial Neural Network (ANN) techniques - Generalized Regression Neural Network (GRNN), Radial Basis Function Neural Network (RBFNN) and Backpropagation Neural Network (BPNN) - to predict mine pit wall deformation. The essence is to carefully choose the best AI technique, which is fault and noise tolerant and has a higher generalization ability. In addition, the selected AI method must correctly handle the non-linearity and high parallelism characteristics exhibited by the rock mass component of the monitored mine pit walls. A total of 709-time series datasets recorded in a daily mark interval were used to develop the ANN prediction models. The overall statistical analyses revealed that the RBFNN demonstrated good prediction power and outperformed the BPNN and GRNN by achieving the least *MAPE*, *MSE*, *RMSE* and the highest *R* and R^2 values of 0.149009%, 0.035698 mm, 0.188939 mm, 0.999984 and 0.999968, respectively.

Keywords: Mining, Mine Deformation, Artificial Intelligent, Artificial Neural Network, Time series.

1 Introduction

Deformation or changes occur in a rock mass when there is continuous but necessary excavation, which is typical in any surface or underground mining activities and other constructional works. These constant activities cause stress in the rock mass of interest, potentially leading to the deformation or instability of structures and mine pit walls. Vicovac *et al*. (2010) underscored that rock falls and landslides (deformation) are the major types of hazards worldwide that can kill or injure many individuals and affect productivity leading to high operational costs. Dick *et al*. (2014) explained that the deformation of mined ground is the earliest and most obvious characteristic of a mine disaster. This problem has necessitated the need for researchers to adopt various mathematical techniques to monitor and predict pit wall deformation (Konakoğlu and Gökalp, 2017). Notable methods include but are not limited to the Pelzer approach, Karlsruhe model, Iterative Weighted Similarity Transformation (IWST), Least Absolute Sum (LAS), Finite Element Method (FEM), inverse velocity (Fukuzono, 1985) and slope gradient (Mufundirwa *et al*., 2010). The last two methods (inverse velocity and slope gradient) are based on the analysis of point measurement data derived from traditional geodetic prism monitoring (Dick *et al*., 2013). It is important to note that researchers (Palazzo *et al*., 2006; Kalkan *et al*., 2010; Osasan and Afeni, 2010) have reviewed the traditional numerical and statistical techniques for predicting structural deformations. However, these techniques are without inhibiting limitations considering the non-linearity and complex nature of structures associated with open-pit mines (Newcomen and Dick, 2016).

Over the years, scholars have relied on more robust Artificial Intelligence (AI) techniques to serve as an alternative to the traditional deformation modelling methods. AI techniques such as Support Vector Machine (SVM), Generalised Regression Neural Network (GRNN), Extreme Learning Machine (ELM), Backpropagation Neural Network (BPNN), Adaptive Neuro-Fuzzy Inference System (ANFIS), Group Method of Data Handling (GMDH) and Radial Basis Function Neural Network (RBFNN)

have been successfully applied to solve multivariate non-linear prediction problems for deformation studies in dams, viaducts, bridges and other edifices (Du *et al*., 2019; Miao *et al*., 2018; Du *et al*., 2013; Sunwen *et al*., 2019; Cheng and Xiong 2017; Armaghani *et al*., 2020; Gourine *et al*., 2012; Lai *et al*., 2015). A general conclusion from these studies indicates that AI models can serve as a benchmark for effective deformation prediction with characters of non-linearity, high parallelism and fault tolerance.

As enumerated, several AI techniques abound for wall forecasting, focusing much on constructional and civil structures other than active mining pit walls. Few scholars, such as Ziggah *et al.* (2018), attempted to predict open pit geodetic deformation using Artificial Neural Networks (ANNs). Du *et al*. (2019) also proposed an ensemble learner which aggregated a set of weaker learners to mine a ground-based interferometric radar to develop a slope deformation prediction model.

This study considered point measurement data derived from individually mounted traditional geodetic prisms on the open pit mine high wall. Monitoring and predicting individual prism displacements is imperative since deformation mostly starts from a localized point. Additionally, the relevance of using point measurement data is attested as it forms the base of analyses when implementing the inverse velocity and slope methods for deformation prediction (Dick *et al.*, 2014). Taking a cue from other monitoring structures, Ziggah *et al*. (2021) concluded that it is not prudent to rely on a unified prediction model where all the data from the mounted prisms, in this case, are combined. Furthermore, to satisfy safety and legal requirements in every mine, monitoring the performance of pit walls cannot be compromised hence the need to develop a prediction model for each mounted prism. This will ultimately lead to minimising property damage, loss of life and operations coming to a halt, which might have dire economic consequences.

Even though AI methods are generally robust compared to the traditional statistical regression methods, each method has some limitations depending on the level of noise tolerance in the data it can accommodate. Moreover, in theory, a specific AI method may be only effective for a particular task and once the research object changes, the prediction performance may degrade drastically (Li *et al*., 2019; Du *et al*., 2019). This confirms the no-free-lunch theorem proposed by Wolpert (1996).

Therefore, the present study was conducted to assess the accuracy performances of three ANN techniques, namely, BPNN, RBFNN and GRNN, for predicting open pit mine wall deformation. These methods have received comprehensive coverage for other structural deformation predictions with accurate results. However, very little application is known in the mine pit wall studies, hence, the option of employing the three ANN methods as mentioned earlier.

2. Study Area and Data Description

2.1 Study Area

The study was conducted on the eastern high wall formation of Mine X. This forms part of a concession of a gold mine company in Tarkwa and lies within latitude 5^0 15' N and longitude 2^0 00' W. Mineralized concentration zone along the hanging (high) wall is proven to be of the highest conglomerate band in the Basal reef. The open pit mine operations exploit narrow, tabular auriferous conglomerates within the paleo placer deposit of the banket series of the Tarkwaian basin. The wall understudy is expected to suit a design of an 18-metre and 6-metre berm and bench formation. Currently, it stretches to about 1 500 metres north-south direction with a total average height of 108 metres, from crest to toe (Fig. 1).

Fig. 1 Mine X Active Mining Pit Wall

2.2 Data Description

A geodetic technique for measuring and assessing deformation was applied to ensure good pit health and safety of operations. The prism monitoring system consists of the base station (where the robotic total station is mounted and reads up to four decimal places), the reference prism (back site) and the monitoring prisms (fixed on the various block or slope elevations being monitored) were applied. Data collection from the prism survey was recorded in the northing (N), easting (E) and elevation (Z) coordinates using the robotic total station mounted on the stationary base station. To a more considerable extent, the coordinates observed determine the increment in magnitude and the rate of deformation, hence their use for model development and prediction. The observational time was also recorded. To minimise the effect of adverse

weather conditions and maintain a uniform temperature, observations were done in the mornings and at sunsets. The study was conducted on a prism labelled P1 mounted on a 71 m reduce-level bench. A total of 709 time series datasets recorded from 6th December 2018 to 14th November 2020 in a daily mark interval were used in this study to develop the ANN displacement prediction models.

3. Methods Used

This study applied and compared three supervised Artificial Neural Network (ANN) techniques of GRNN, RBFNN and BPNN to predict mine pit wall deformation. Each of these model techniques was developed in the MATLAB environment. A brief description of the methods is presented in the subsequent sections.

3.1 The Back Propagation Neural Network

This ANN approach consists of neurons (computational processors) that are connected and operate in parallel and learn from experience.

The BPNN used in this study is a supervised multilayer feedforward network with a non-linear activation function consisting of input, hidden, and output layers (or neurons) (Fig. 2), with each neuron receiving a weighted sum from interconnected neurons. It has a proven record of learning fast and can handle relatively small datasets. The activation function usually used in the hidden layer is the sigmoid function, even though there are others, such as rectified linear unit, softplus and hyperbolic tangent (Szandala, 2020).

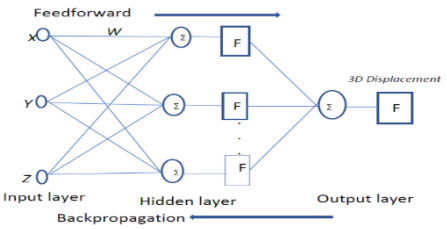

Fig. 2 BPNN structure with 3 input variables for predicting mine pit wall deformation

In the BPNN, the error computed at the output is propagated backwards through the layers to update the weights and biases. The steps used in calculating the backpropagation as described by Miima *et al.* (2001) is presented as follows:

1. Select the number of input neurons (n), output neurons (q) and hidden neurons (m). Present continuous valued vector for the first training example (x_i);

$$\{X_i\} = \begin{bmatrix} x_1 \\ x_2 \\ \vdots \\ x_n \end{bmatrix}$$

2. Initialize all the weights to small random values$[W_n]$
3. Compute the value $\{net_j\}$ for hidden layers;

$$\{net_j\} = \begin{Bmatrix} net_1 \\ net_2 \\ \vdots \\ net_m \end{Bmatrix} = [W_n]\{x_i\}$$

4. Calculate the activation value$\{out_j\}$ for hidden layers using for example, the sigmoid logistic activation function f (.) with a threshold parameter θ_j.

$$\{out_j\} = \begin{Bmatrix} f_{1(net_1)} \\ f_{1(net_2)} \\ \vdots \\ f_{m(net_{m1})} \end{Bmatrix}$$

$$= \begin{Bmatrix} 1/(1+e^{(-net_1+\theta_1)}) \\ 1/(1+e^{(-net_2+\theta_2)}) \\ \vdots \\ 1/(1+e^{(-net_m+\theta_m)}) \end{Bmatrix}$$

5. Calculate the input value $\{net_k\}$ to the output layer;

$$\{net_k\} = [W_{kj}]\{out_j\}$$

6. Calculate the activation value $\{out_k\}$ for the output layer;

$$\{out_j\} = \begin{Bmatrix} y_1 \\ y_2 \\ \vdots \\ y_p \end{Bmatrix} = \begin{Bmatrix} f_1(net_1) \\ f_2(net_2) \\ \vdots \\ f_q(net_q) \end{Bmatrix}$$

$$= \begin{Bmatrix} 1/(1+e^{(-net_1+\theta_1)}) \\ 1/(1+e^{(-net_2+\theta_2)}) \\ \vdots \\ 1/\left(1+e^{(-net_q+\theta_q)}\right) \end{Bmatrix}$$

7. Calculate error $[W_{kj}]$;

$$[W_{kj}] = n\{Y_k - y_k\}\{y_k\}\{out_j\}^T + \propto [\Delta_g W_{kj}]$$

with α and *n* the learning rate and momentum terms respectively.

8. Compute the new values of weights between the hidden and the output layers

$$[W_{kj}] = [W_{kj}] + [\Delta W_{kj}]$$

9. Calculate the $[\Delta W_n]$for the input to hidden weights

$$[\Delta W_{ji}] = n\{out_j\}\{Y_k - y_k\}\{y_k\}.\{W_{kj}\}^T\{x_i\}^T + \propto [\Delta_q W_{ji}]$$

10. Calculate the new values of weights between the input and hidden layer

$$[W_{ji}] = [W_{ij}] + [\Delta W_n]$$

11. Repeat by going to step 3 for all learning sample until the set stopping criteria is achieved

The dataset was divided into training and testing datasets to ensure network generalization and accuracy. As a rule of thumb, the majority (80%, constituting 567) of the dataset was selected for the training. The dataset was not chosen randomly because the data observed was recorded in time series. The remaining 20% (142) formed the testing dataset to authenticate the model's efficacy.

The input and output data were fed into the network. After several iterations (epochs), the network parameters such as learning rate, momentum, and weights were updated until learning was successful; that is, a minimal error was achieved.

3.2 The Radial Basis Function Neural Network

The RBFNN is a three-layer feedforward network that consists of an input layer, a hidden layer and an output layer (Fig. 3). It is classified as a universal function approximator is trained by using supervised training algorithm (Wu *et al*. 2012). The RBFNN is a three-layer feedforward network consisting of an input layer, a hidden layer and an output layer (Fig. 3). It is classified as a universal function approximator and are trained by is trained using supervised training algorithm.

The input layer receives projected grid coordinates (Easting, Northing, Elevation) from the environment are received by the input layer and then transmitted as data to the hidden layer. The hidden layer containing the activation function performs the non-linear transformation of the inputs (Easting, Northing, Elevation). In this study, the Gaussian function was used as the radial basis function in the hidden layer, and this was defined by methods such as clustering or the orthogonal least squares (OLS) method. The output layer is a linear combiner, mapping the non-linearity into a new space, and constitutes the 3-dimension displacement (deformation). The research applied the OLS algorithm in MATLAB for modelling the output.

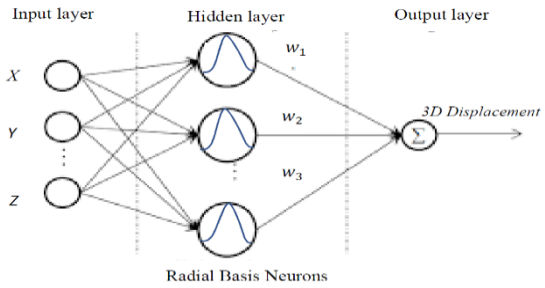

Fig. 3 RBFNN structure with 3 input variables for predicting mine pit wall

The summation of output of hidden layers with some weight is then provided as the output of the RBFNN.

3.3 The Generalised Regression Neural Network

The GRNN constitutes a single-pass neural network based on general regression theory. It uses the Gaussian activation function in the hidden layer as the function approximator. The network architecture of GRNN is made up of the input, hidden, summation and output layers (Fig. 4). As with other networks; the input layer receives the inputs from the datasets. The pattern layer calculates the Euclidean distance. Next is the summation layer, which constitutes the numerator (N) and denominator (D) parts. When applying GRNN, the spread constant comprises the adjustable parameter that needs to be fine-tuned. The output is estimated using the weighted average of the training dataset's outputs, where the weight is calculated using the Euclidean distance between the training data and test data. For this study, three variables (E, N, Z) were used as the input variables to train and test the model, while the output was the 3D displacement. The model was developed in the MATLAB environment.

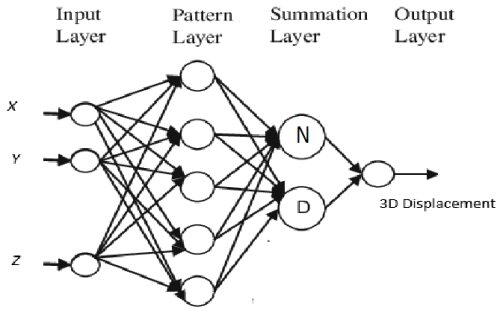

Fig. 4 GRNN structure with 3 input variables for predicting mine pit wall deformation

3.4 Model Architecture and Statistical Evaluators

The network's architectural design is vital in analysing and accurately predicting the pit wall 3D displacement. The BPNN, RBFNN and GRNN models were developed with the observed Easting, Northing and Elevation serving as the input variables and their corresponding 3D displacement as the output. In all, a total of 709 epochs of observations were recorded. In building the models, datasets were normalized into intervals -1 and 1 to eliminate redundant data and obey the Gaussian distribution curve. As a rule of thumb, the datasets were divided into training and testing datasets using the hold-out cross-validation approach, with 567 (80%) constituting the training set and 142 (20%) for the testing set. The efficacy of each model was determined using the testing datasets, which provide information about the ability to generalise with minimal error. It must be noted that the sampling of datasets was in a time series approach, and hence a random sample was not appropriate.

Each model was tested using statistically proven evaluators such as the mean absolute percentage error (MAPE), mean square error (MSE), root mean square error (RMSE), correlation coefficient (R) and coefficient of determination (R^2). Statistically, relatively low MAPE, MSE and RMSE values are accepted, and the model is considered a good predictor. Low RMSE and MSE values also indicate fewer residual errors recorded by a model. The *R* and R^2 quantify the strength of linear relationships between the actual and observed 3D deformation values of each model. A close to unity indicates the most vital relationship. When the actual individual values are selected, the corresponding predicted values could replicate the historical datasets. This further shows that the predicted values move in the same direction and magnitude in a time series manner. Equations (1) to (4) give the mathematical expressions of the evaluators (Temeng *et al*., 2020).

$$\mathrm{MAPE} = (100\%/\mathrm{N})\sum_{\mathrm{i}=1}^{\mathrm{N}}|(\mathrm{M_i} - \mathrm{P_i})/\mathrm{M_i}| \quad (1)$$

$$\mathrm{RMSE} = \sqrt{(1/\mathrm{N})\sum_{\mathrm{i}=1}^{\mathrm{N}}(\mathrm{M_i} - \mathrm{P_i})^2} \quad (2)$$

$$MSE = \frac{1}{n}\sum_{i=1}^{n}(M_i - P_i)^2 \quad (3)$$

$$R = \frac{\left(\sum_{\mathrm{i}=1}^{\mathrm{N}}(\mathrm{M_i} - \bar{\mathrm{M}})(\mathrm{P_i} - \bar{\mathrm{P}})\right)}{\left(\sqrt{\sum_{\mathrm{i}=1}^{\mathrm{N}}(\mathrm{M_i} - \bar{\mathrm{M}})^2} \times \sqrt{\sum_{\mathrm{i}=1}^{\mathrm{N}}(\mathrm{P_i} - \bar{\mathrm{P}})^2}\right)} \quad (4)$$

M_i and P_i represent the observed and predicted 3D deformation values. The arithmetic mean for the observed and predicted values are represented by $\bar{\mathrm{M}}$ and $\bar{\mathrm{P}}$. R^2 can be calculated by taking the square root of *R*.

4. Results and Discussion

4.1 BPNN Model Performance

The Levenberg-Marquardt learning algorithm (Ziggah *et al*., 2021; Arthur *et al*., 2020) was applied to train the network. A momentum coefficient of 0.8 and a learning rate of 0.03 were applied during the training process. The hyperbolic tangent activation function was used in the hidden layer, while the linear activation function was used in the output layer since the dataset observed satisfies a regression problem. As a rule of thumb, the optimal hidden neurons based on the least *RMSE* for the model testing was chosen using a trial-and-error approach. For the 3D displacement prediction, the optimal BPNN architecture consisted of three inputs, one hidden layer with twenty-seven optimal neurons and one output layer thus, [3-27-1].

The validity of the BPNN was tested using various statistical indicators such as the *RMSE, MAPE, MSE, R* and R^2. Table 1 shows the matrix presentation of the multiple evaluators for the performance. It is observed that the BPNN model produced good values of *RMSE, MSE, R,* R^2 and *MAPE*. Based on the reported results, it can be inferred that the 3D displacement prediction by the BPNN model on the test datasets does not deviate significantly from the measured values. Again, high *R* and R^2 values approaching unity indicate a strong correlation between the observed and predicted values for the BPNN model. This makes BPNN to be a preferred model for pit wall deformation prediction.

Table 1 BPNN Model Performance Results for Training and Testing Datasets

Performance Indicators	Training	Testing
MAPE (%)	0.443524	0.207612
MSE (mm)	0.439366	0.075088
RMSE (mm)	0.662847	0.274021
R	0.999813	0.999963
R^2	0.999627	0.999926

4.2 RBFNN Model Performance

In defining the RBFNN training model, more than one hyperparameter tuning was required to achieve optimal results. The RBFNN optimal solution leading to a smooth function was reached after several training trials with a spread parameter value of 0.8 and a maximum number of neurons set at 70. As shown in Table 2, there is a close to perfect relationship between the observed and predicted output datasets. This is further indicated by the higher *R* and R^2 statistical measurements recorded (Table 2) for the training and testing datasets. Furthermore, the error figures recorded in the training and testing results are relatively small, as recorded by the *MAPE, RMSE* and *MSE* statistical indicators. Hence, values predicted by the RBFNN model are very close to the observed values.

Table 2 RBFNN Model Performance Results for Training and Testing Datasets

Performance Indicators	Training	Testing
MAPE (%)	0.572501	0.149009
MSE (mm)	0.078542	0.035698
RMSE (mm)	0.280254	0.188939
R	0.999967	0.999984
R^2	0.999933	0.999968

4.3 GRNN Model Performance

GRNN modelling can be successful when applying appropriate spread or smooth factors (Bachir *et al*., 2012). The spread parameter optimum value was determined after a series of iterations, and in this study, 0.05 was the optimal number since it yielded minimal error values. The effectiveness of the GRNN model is presented in Table 3. GRNN model statistically yielded *R* and R^2 values indicating a good relationship between the predicted and actual results. The model also generated RMSE, MAPE and MSE values that indicate acceptable prediction performance.

Table 3 GRNN Model Performance Results for Training and Testing Datasets

Performance Indicators	Training	Testing
MAPE (%)	1.000341	3.14266
MSE (mm)	0.902378	12.21809
RMSE (mm)	0.949936	3.495438
R	0.999617	0.993564
R^2	0.999234	0.98717

4.4 Comparing BPNN, RBFNN and GRNN Results

The ranking effectiveness of the models applied-BPNN, RBFNN and GRNN are compared using RMSE, MAPE, MSE, *R* and R^2. Tables 4 and 5 provide the best option for evaluating the model-predicted 3D point deformation on the mine pit wall. Tables 4 and 5 show that the model with the lowest RMSE recorded indicates the best absolute fit to the data. It can be observed in Table 5 that the RBFNN model yielded the best RMSE test value of 0.1889387 mm, followed by BPNN and GRNN with 0.274021 mm and 3.4954381 mm. This can be confirmed in Fig. 5

The MAPE indicator expresses the accuracy of the predictive models as a percentage of the error. Tables 4 and 5 indicate competitive MAPE test results of 0.207611928% and 0.149009029% for BPNN and RBFNN models, respectively (Fig. 6). In effect, RBFNN could interpret about 99.850991% of the data variations. In comparison, the BPNN model could interpret 99.792388% of the data variations. The worst-performing testing model in MAPE was the GRNN, recording a 3.1426595% of error deviation of the predicted output from the actual output. Thus, about 96.8573405% of the data variations could be interpreted by the GRNN model.

The MSE is commonly used in machine learning to represent the error loss function and indicates how close the regression line is to the set of points. The lower the MSE value, the better the model. Tables 4 and 5 show minimal MSE test values of 0.07508759 mm and 0.035697844 mm for BPNN and RBFNN models, indicating better predictive models. Comparatively, from the testing results, the RBFNN model recorded about 50% superior strength over the BPNN in terms of the MSE evaluator, with GRNN performing poorly in that regard.

The *R* is the degree of relationship between the observed values and the predicted values. It is observed that RBFNN, BPNN and GRNN recorded high and close *R* values above 0.9, representing a good relationship between the observed and predicted values (Fig. 7). However, the best

correlation was observed for the RBFNN model as it recorded test values of 0.9999839 and 0.9999678 for both R and R^2, respectively. This implies that the RBFNN predictions exhibit higher replication on the historical datasets.

Table 4 Statistical Training Results for the various ANN models

Method	Statistical Performance indicators (training)				
	MAPE (%)	MSE (mm)	RMSE (mm)	R	R^2
BPNN	0.443524	0.439366	0.662847	0.999813	0.999627
RBFNN	0.5725012	0.0785421	0.2802537	0.9999666	0.9999331
GRNN	1.0003409	0.9023782	0.9499359	0.9996168	0.9992338

Table 5 Statistical Testing Results for the various ANN models

Method	Statistical Performance indicators (testing)				
	MAPE (%)	MSE (mm)	RMSE (mm)	R	R^2
BPNN	0.207612	0.075088	0.274021	0.999963	0.999926
RBFNN	0.149009	0.0356978	0.1889387	0.9999839	0.9999678
GRNN	3.1426595	12.218088	3.4954381	0.9935642	0.9871697

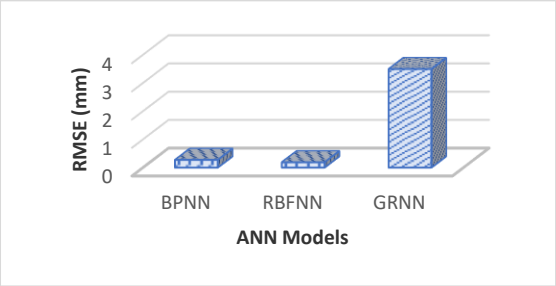

Fig. 5 RMSE analysis

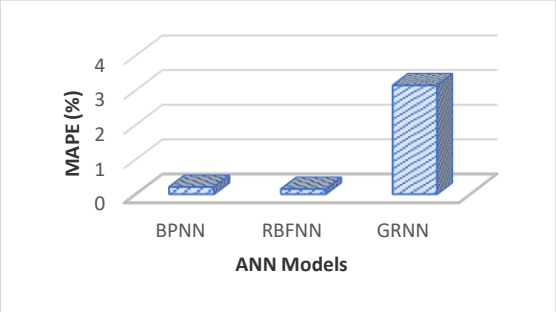

Fig. 6 MAPE analysis

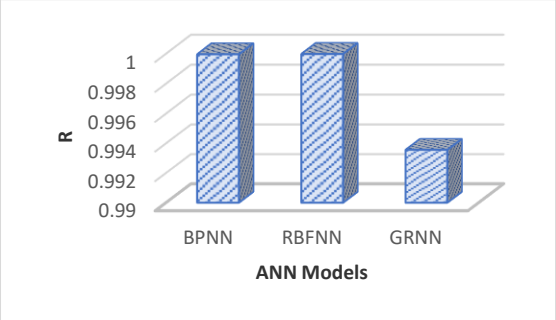

Fig. 7 Coefficient of Correlation (R) analysis

5. Conclusions and Recommendations

The study assessed the accuracy performances of three supervised AI methods of BPNN, RBFNN and GRNN as viable tools for predicting 3D deformation on an active mine pit wall. The statistical evaluators indicate that all the models considered had good predictive strength. The overall statistical analyses, however, revealed that the RBFNN demonstrated good prediction power and outperformed the BPNN and GRNN by achieving the least MAPE, MSE, RMSE and the highest R and R2 values of 0.149009%, 0.035698 mm, 0.188939 mm, 0.999984 and 0.999968, respectively. Due to the increased risk and sensitive nature of mine pit walls which has become a safety concern, it is prudent to adopt the best predictive model and explore other hybrid techniques. In addition to using a point source (prism monitoring system) for surface displacement data collection, other sources, such as radar monitoring techniques, can be explored and combined to provide further understanding in deformation studies.

References

Armaghani, D. J., Momeni, E. and Asteris, P. G. (2020), "Application of Group Data Handling Technique in Assessing Deformation of Rock Mass", Metaheuristic Computing and Applications (MCA) Journal, 1p.

Arthur, C. K. Temeng, V. A. and Ziggah, Y. Y. (2020), "Performance Evaluation of Training Algorithms in Backpropagation Neural Network Approach to Blast-induced Ground Vibration Prediction", *Ghana Min J*. vol 20, pp. 20 - 23.

Bachir, G., Mahi, H., Khaoudiri, A. and Laksari, Y. (2012), "The GRNN and the RBF Neural Networks for 2D Displacement Field Modelling", Case Study: GPS Auscultation Nertwork of LNG Reservoir (GL4/Z Industrial Complex – Arzew, Algeria), pp. 2 – 18.

Cheng, J. and Xiong, Y. (2017), "Application of Extreme Learning Machine Combination Model for Dam Displacement Prediction", *International Congress of Information and Communication Technology (ICICT), Procedia Computer Science*, pp. 1- 6.

Dick, G., Erik, E., Albert, G., Doug, S. and Nick, D. (2014), "Development of an Early Warning Time-of-Failure Analysis Methodology for Open-pit Mine Slopes Utilizing Ground-Based Slope Stability Radar Monitoring Data", *Can. Geotech. J.* p. 52, 515 - 529.

Du, J., Yin, K., Lacasse, S. (2013), "Displacement Prediction in Colluvial Landslides", *Three Gorges Reservoir, China, Landslides* 10 (2), pp. 203 - 218.

Du, S., Feng, G., Wang, J., Feng, S., Malekian, R. and Li, Z. (2019), "A New Machine-Learning Prediction Model for Slope Deformation of an Open-Pit Mine: An Evaluation of Field Data", *Energies*, pp. 1 - 15.

Fukuzono, T. (1985), "A New Method for Predicting the Failure Time of a Slope", *Proceedings of the 4th International Conference and Field Workshop on Landslides, Tokyo*: Tokyo University Press, pp. 145 – 150.

Gourine, B., Mahi, H., Khoudiri, A. and Laksari, Y. (2012), "The GRNN and the RBF Networks for 2D D isplacement Field Modeling", Case Study: *GPS Auscultation Network of LNG Reservoir (GL4/Z) Industrial Complex – Arzew, Algeria, FIG*, pp. 2 - 15.

Kalkan, Y., Reha, M., Alkan, R. M. and Bilgi, S. (2010), "Deformation Monitoring Studies at Atatürk Dam", *FIG, Congress, Facing the Challenges- Building the Capacity*, Sydney, Australia, 11-16 April, 14p.

Konakoğlu, B. and Gökalp, E. (2017), "Deformation Measurements and Analysis with Robust Methods: A Case Study, Deriner Dam", *Turkey Journal of Science and Technology*, vol. 13(1), pp. 99 - 103.

Lai, J., Qiu, J., Feng, Z., Chen, J. and Fan, H. (2015), "Prediction of Soil Deformation in Tunnelling Using Artificial Neural Networks", *Computational Intelligence and Neuroscience, vol. 2016, access: www.hindawi.com.*

Li, Z., Goebel, K., Wu, D. (2019), "Degradation Modelling and Remaining Useful Life Prediction of Aircraft Engines Using Ensemble Learning", *J. Eng. Gas Turbines Power-Trans. ASME*, pp. 141, 041008.

Miao, F., Wu, Y., Xie, Y., Li., Y. (2018), "Prediction of Landslide Displacement with Step-Like Behaviour Based on Multialgorithm Optimisation and a Support Vector Regression Model", *Landslides*, 15 (3), pp. 475 - 488.

Miima J. B., Niemeier, W. and Kraus, B. (2001), "A Neural Network Approach to Modelling Geodetic Deformations", *First International Symposium on Robust Statistics and Fuzzy Techniques in Geodesy and GIS*, Zurich, pp. 111 - 115.

Mufundirwa, A., Fujii, Y., Kodama, J. (2010), "A New Practical Method for Prediction of Geomechanical Failure-Time", *Int. J. Rock Mech. Min. Sci*. 47(7), pp. 1079 - 1090.

Newcomen, W. and Dick, G. (2016), "An Update to the Strain-based Approach to Pit Wall Failure Prediction and a Justification for Slope Monitoring", *Journal of The South African Institute of Mining and Metallurgy",* pp. 1 – 7.

Osasan, S.K. and Afeni, T. B. (2010), "Review of Slope Monitoring Techniques", *Journal of Mining Science*, Vol. 46, No. 2, pp. 177 - 186.

Palazzo, D., Friedman, R., Nadal, C., Santos-Filho, M., Viega, L. and Faggion, P. (2006), "Dynamic Monitoring of Structures Using a Robotic Total Station", *XXIII FIG Congress*, Munich, Germany, Oct. 8-13, 10pp.

Sunwen, D., Feng, G., Wang, J., Feng, S., Malekian, R. and Li, Z. (2019), "A New Machine-Learning Prediction Model for Slope Deormation of an Open-Pit Mine: An Evaluation of Field Data", *Energies*, 2019, 12, 1288, pp. 1 - 14.

Szandala, T. (2020), "Review and Comparison of Commonly Used Activation Functions for Deep Neural Networks", Wroclaw University of Science and Technology, Wroclaw, Poland. Retrieved from *www.arxiv.org*.

Temeng, V.A., Ziggah, Y.Y. and Arthur, C.K. (2020), "A Novel Artificial Intelligent Model for Predicting Air Over Pressure Using Brain Inspired Emotional Neural Network",

International Journal of Mining Science and Technology, pp. 1 - 7.

Vicovac, T., Reiterer, A., Egly, U., Eiter, T. and Rieke-Zapp, D. (2010), "Intelligent Deformation Interpretation", *Second International Workshop (AIEG 2010)*, Braunschweig, Germany, pp. 10 - 19.

Wolpert, D. H. (1996), "The lack of a priori distinctions between learning algorithms", *Neural computation*, Vol. 8, No. 7, pp.1341 - 1390.

Wu, Y., Wang, H., Zhang, B. and Du, K. L. (2012), "Using Radial Basis Function Networks for Function Approximation and Classification", *International Scholarly Research Notices*, *Hindawi*, Vol. 2021, Article ID 324194.

Ziggah, Y. Y., Hu, Y., Issaka, Y. and Laari, P. B. (2019), "Least Square Support Vector Machine Model for Cordinate Transformation", *Geodesy and Cartography*, 45(1), pp. 16 - 27.

Ziggah, Y.Y., Issaka, Y. and Laari, P.B. (2021), "Evaluation of Different Artificial Intelligent Methods for Predicting Dam Piezometric Water Level", *Modelling Earth Systems and Environment*, pp. 1 - 16.

Authors

Ebenezer Kofi Apraku works with Gold Fields Ghana Limited and is a PhD candidate in Geomatic Engineering with the University of Mines and Technology (UMaT), Tarkwa. He holds a BSc, MSc and MPhil degrees in Geomatic and Mining Engineering from UMaT. His research interests are in the fields of AI, mine operations and deformation modelling.

Yao Yevenyo Ziggah is a Senior Lecturer with the Geomatic Engineering Department, University of Mines and Technology, Tarkwa. He received his BSc (Hons.) in Geomatic Engineering from the Kwame Nkrumah University of Science and Technology (KNUST), Kumasi, Ghana, and MEng and PhD in Geodesy and Survey Engineering from the China University of Geosciences (CUG), Wuhan, P. R. China, respectively. His research interests include the application and development of artificial intelligence in geoscience and engineering, fractal analysis, 2D/3D coordinate transformation, height systems, gravity field modelling, and geodetic deformation modelling.

Bernard Kumi-Boateng is a Professor with the Geomatic Engineering Department, University of Mines and Technology, Tarkwa, Ghana. He holds a BSc degree in Geomatic Engineering from Kwame Nkrumah University of Science and Technology (KNUST), Kumasi, Ghana. He obtained his Master of Science degree and Doctor of Philosophy from the International Institute for Geo-Information Science and Earth Observation (ITC), Enschede-The Netherlands and UMaT respectively. His research interests include Resettlement Action Plan (RAP), application of Remote Sensing and GIS in Environmental Management, Spatial Statistics, Land and Compensation Surveys and Urban Mining (E-Waste) Strategy.